ADVANCED ELECTRONIC MATERIALS
www.advelectronicmat.de

# Mechanism of Spin-Orbit Torques in Platinum Oxide Systems

*Jayshankar Nath,* Alexandru Vladimir Trifu, Mihai Sebastian Gabor, Ali Hallal, Stephane Auffret, Sebastien Labau, Aymen Mahjoub, Edmond Chan, Avinash Kumar Chaurasiya, Amrit Kumar Mondal, Haozhe Yang, Eva Schmoranzerova, Mohamed Ali Nsibi, Isabelle Joumard, Anjan Barman, Bernard Pelissier, Mairbek Chshiev, Gilles Gaudin, and Ioan Mihai Miron**

**Spin-Orbit Torque (SOT) Magnetic Random-Access Memories (MRAM) have shown promising results toward the realization of fast, non-volatile memory systems. Oxidation of the heavy-metal (HM) layer of the SOT-MRAM has been proposed as a method to increase its energy efficiency. But the results are widely divergent due to the difficulty in controlling the HM oxidation because of its low enthalpy of formation. Here, these differences are reconciled by performing a gradual oxidation procedure, which allows correlating the chemical structure to the physical properties of the stack. As an HM layer, Pt is chosen because of the strong SOT and the low enthalpy of formation of its oxides. The evidence of an oxide inversion layer at the ferromagnet (FM)/HM interface is found: the oxygen is drawn into the FM, while the HM remains metallic near the interface. Moreover, the oxygen migrates in the volume of the FM layer rather than being concentrated at the interface. Consequently, it is found that the intrinsic magnitude of the SOT is unchanged compared to the fully metallic structure. The previously reported apparent increase of SOTs is not intrinsic to platinum oxide and instead arises from systemic changes produced by oxidation.**

J. Nath, A. V. Trifu, A. Hallal, S. Auffret, E. Chan, H. Yang, E. Schmoranzerova, M. A. Nsibi, I. Joumard, M. Chshiev, G. Gaudin, I. M. Miron
SPINTEC
UMR-8191
CNRS/CEA/Université Grenoble Alpes
Grenoble 38054, France
E-mail: jsnath@ucla.edu; mihai.miron@cea.fr

M. S. Gabor
C4S
Physics and Chemistry Department
Technical University of Cluj-Napoca
Cluj-Napoca 400114, Romania

S. Labau, A. Mahjoub, B. Pelissier
Université Grenoble Alpes
CNRS, CEA/LETI Minatec, LTM
Grenoble 38054, France

A. K. Chaurasiya, A. K. Mondal, A. Barman
Department of Condensed Matter Physics and Material Sciences
S. N. Bose National Centre for Basic Sciences
Kolkata 700106, India

M. Chshiev
Institut Universitaire de France (IUF)
Paris 75231, France

The ORCID identification number(s) for the author(s) of this article can be found under https://doi.org/10.1002/aelm.202101335.

**DOI: 10.1002/aelm.202101335**

## 1. Introduction

The process of transferring data between the memory and logic elements of a computer is one of the most energy intensive steps and is a bottleneck in terms of speed. Before moving to unconventional architectures such as "logic-in-memory" or "machine learning systems," the most direct solution seems to be to include non-volatility in the memory hierarchy. For that, the spin-orbit torque (SOT) magnetic random-access memory (MRAM)[1] is the only non-volatile memory technology that can function at the speed of the processors (at least at GHz). This memory is targeted toward replacing the current Complementary Metal-Oxide-Semiconductor (CMOS) based Static RAMs (SRAM) and Dynamic RAMs (DRAM), with a greater emphasis on key metrics such as energy efficiency, non-volatility, speed, size, and endurance.

In SOT-MRAM, a current injected into the heavy-metal (HM) layer with high Spin-Orbit Coupling (SOC) gives rise to the Damping-Like (DL) and the Field-Like (FL) torques. These torques act on the magnetization of the adjacent ferromagnet (FM) layer to switch it during the write operation.[2,3] The main figure of merit of SOT-MRAM is the switching current, which dictates the power consumption as well as the footprint of the transistors that drives the memory cell.[4]

Numerous works have been published, engineering either the bulk of the HM or the FM/HM interface to reduce the writing current: from using resistive HMs[3,5–7] to alloying[8,9] in the case of bulk methods and using insertion layers[10–12] and spin sinks[13,14] in case of interfacial methods. One particularly attractive method to enhance the SOT is to oxidize the HM.[15–19] Its main advantage is that the SOT created at the Oxide/FM interface could be stronger than the SOT from the HM, while also consuming less current, due to the insulating nature of the oxide. While most of the published works on this topic report an increase of the SOT efficacy, there is an ongoing debate as some other studies do not observe such a clear improvement.[20] This ambiguity in the experimental results published so far necessitates a clear study of HM oxide systems, as this issue is highly relevant from a technological perspective in the development of SOT-MRAMs.

 

## 2. Generation of SOTs by the Oxidized Platinum Layer

In this work, we study the SOTs generated by oxidizing the platinum layer in a Ta(3 nm)/Cu(1 nm)/Co(2 nm)/Pt(4–1 nm) multilayer stack to determine the exact contribution of oxidation in these structures. The sample stack is shown in **Figure 1**a. Here, the Cu/Co/Pt forms the inversion asymmetric tri-layer, while the Ta acts as a seed layer. The torques generated by the seed Ta layer were measured using a reference sample of Ta(3 nm)/Cu(1 nm)/Co(2 nm)/Al(2 nm), without the SOT generating Pt layer and the top Al layer acting as the capping layer. These torques were normalized to the electric field and subtracted from the measurement results, to present the effect of Pt oxidation exclusively. Unlike the bulk oxidation of the HM layer during deposition utilized in the previous works,[16–20] the wedge of platinum creates a continuous gradient of oxidation, while all the other properties of the samples remain unchanged. This specificity of the wedge ensures that all our samples are deposited at the same time, avoiding any material differences from sequential deposition runs. The sample was oxidized post-deposition[21] and was coated with Poly(methyl methacrylate) (PMMA) to avoid further atmospheric oxidation.

Devices were fabricated along the Pt wedge and the SOTs were measured using the 2nd harmonic torque measurement technique.[22] The DL fields thus extracted and normalized to the applied current are plotted in Figure 1b. At higher thicknesses of Pt, the unoxidized (UO) and the oxidized (OX) samples generate the same amount of torque. However, at lower thicknesses, the OX samples exhibit an increase in SOTs. This increase, also observed in previous studies, was interpreted as an indicator of SOTs arising from FM/HM interfacial oxidation. Moreover, since oxidation also increases the perpendicular magnetic anisotropy of the FM layer, novel SOT-MRAM devices can be imagined with the FM layer sandwiched between a top MgO layer and a bottom oxidized Pt layer, resulting in enhanced SOTs and perpendicular magnetic anisotropy.

For these reasons, it is critical to determine the precise role of oxygen at the FM/Pt interface. The first step is to determine the distribution of oxygen in the stack and its effect on the physical and electrical characteristics of the Pt layer. This can be ascertained by using the Angle-Resolved X-ray Photoelectron Spectroscopy (AR-XPS) technique plotted in Figure 1c,d. We selected two OX samples at 2 and 1.6 nm of Pt thickness, corresponding to either a negligible effect or a significant increase of SOTs, respectively. Figure 1c displays the Pt spectra of the OX(2) and OX(1.6) samples. Both these samples indicate the presence of excited states of Pt, corresponding to its oxidized states, namely the $Pt^{2+}$ and $Pt^{4+}$. However, comparing the area under the peaks of $Pt^{0+}$ to $Pt^{2+}$ and $Pt^{4+}$, it is evident that OX(1.6) is more strongly oxidized owing to its thinner Pt thickness. Figure 1d displays the Co spectra of these two samples. OX(2) doesn't show any excited states, indicating that the Co is unoxidized. However, OX(1.6) indicates the presence of the excited states corresponding to the oxides of Co, indicating that the oxygen in this sample has reached the Co/Pt interface. The

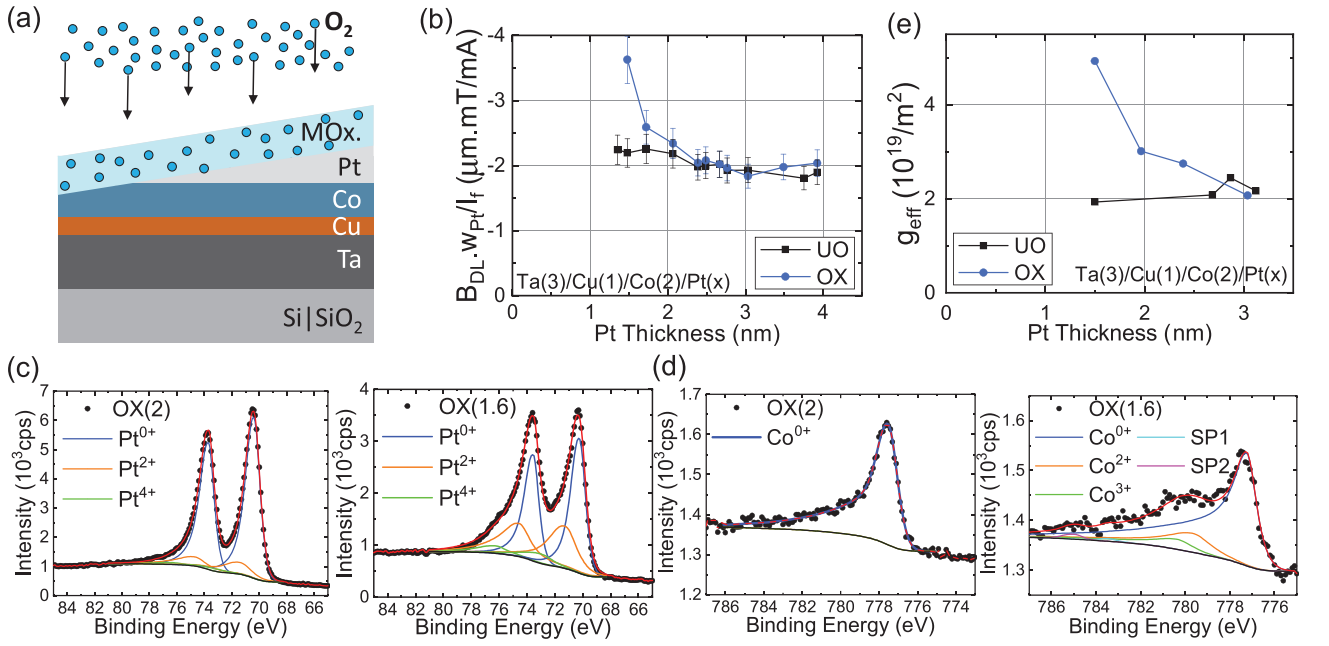


**Figure 1.** a) Schematics of the multilayer stack of Ta(3 nm)/Cu(1 nm)/Co(2 nm)/Pt(4–1 nm). Here, MOx. refers to Metal-Oxide, b) DL field normalized to the applied current. The error in this plot arises primarily from the estimation of the current density, due to microfabrication induced variations. We estimate this error to be less than 10%. c) pAR-XPS Pt spectra (75° acquisition angle) of the OX(2 nm) (left) and OX(1.6 nm) (right) samples. d) Co spectra (75° acquisition angle) of the OX(2 nm) (left) and OX(1.6 nm) (right). In (c) and (d), the black curve corresponds to the baseline spectra and the red line corresponds to the data fit. e) Effective spin-mixing conductance as a function of Pt thickness. UO and OX refer to unoxidized and oxidized samples respectively. Samples UO (1.5 nm, 2.9 nm) of (e) were deposited separately. The error in this plot arises primarily from the quantification of the saturation magnetization, which we estimate to be less than 10%.

correlation between the interfacial oxidation and the increase of SOTs could indicate an enhancement of the Rashba effect[23] as well as a change of the spin mixing conductance of this interface.

To test this hypothesis, we performed the Ferromagnetic Resonance (FMR) measurements on the samples, allowing us to determine the effective spin-mixing conductance, $g_{eff}$, plotted in Figure 1e.[21] This plot indicates that there is an enhancement of spin-mixing conductance at the interface, with interfacial oxidation. Hence, the increase of SOTs, which is an interfacial effect, could also arise from the enhancement of spin-mixing conductance at the interface.[13,24]

Up to this point, the results that we find are in agreement with previous studies,[17,18] reporting an enhancement of the SOT as well as a change of the spin mixing conductance. However, these conclusions are reached with the assumption that the Pt oxide remains stable while in contact with the metallic Co, which is not compatible with the relative enthalpy of formation of these oxides. It is energetically more favorable to form oxides of Co (CoO: −237.9 kJ mol$^{-1}$; $Co_3O_4$: −891 kJ mol$^{-1}$)[25] rather than oxides of Pt ($PtO_2$: −80 kJ mol$^{-1}$; $Pt_3O_4$: −163 kJ mol$^{-1}$).[26] Hence, we need to determine the exact distribution of the oxygen inside the functional stack to understand how the oxidation affects the magnetic properties as well as the electric current flow. We will then correct the measured values of the SOTs to include all the changes of the physical properties.

## 3. Distribution of Oxygen in the Material Stack

In 2nd harmonic torque measurements, we are comparing the action of current to that of the magnetic field. Hence, if the saturation magnetization, $M_S$, varies between the samples, then the extracted SOT field needs to be scaled accordingly. We measured the saturation magnetization using a Vibrating Sample Magnetometry (VSM). These data, after correcting for the Co thickness variation across the wafer,[21] are plotted in **Figure 2**a. Above 1.8 nm of Pt thickness, there is negligible difference between the $M_S$ of the samples. However, below this thickness of Pt, there is a significant drop in $M_S$, indicative of Co oxidation.

When a current is applied in a SOT device, it redistributes itself into the various metallic layers depending on their relative resistivities. However, the majority of the SOTs are generated in the functional Pt layer. To determine the current flowing within the Pt layer, we need to quantify the conductance of the layers. These were measured using the 4-point resistance measurement technique and the data fit with the Fuchs-Sondheimer (FS) model,[21,27,28] with results presented in Figure 2b. Because the Pt thicknesses here are smaller than the mean free path of electrons in the metal, we cannot extract meaningful values for all the physical parameters in the model. However, because the model fits the data sufficiently well, by extrapolating to zero thickness, we can determine the conductance of the layers underneath Pt.[21] The conductance

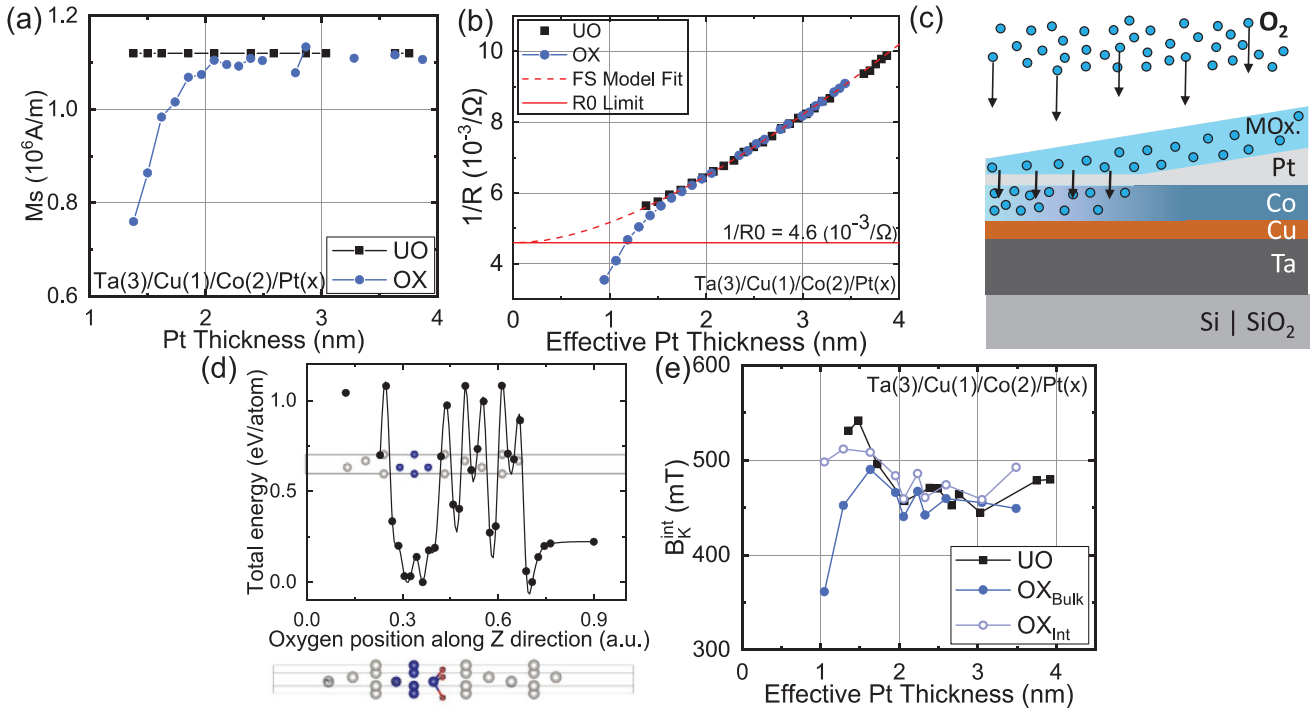


**Figure 2.** a) Saturation magnetization of UO and OX samples. b) Dependence of the conductance on the effective platinum thickness. The dashed line corresponds to the Fuchs-Sondheimer fit and the red line corresponds to the conductance of the layers underneath Pt. c) Schematic of the proposed model illustrating the oxygen pumping into the Co layer. d) The energy of the system (black dots) depending on the placement of the oxygen atoms in the lattice, determined using ab-initio calculations. The blue dots correspond to the Co atoms and the white dots correspond to the Pt atoms in the lattice. The bottom frame corresponds to the scenario when oxygen (red dots) is placed at the Co/Pt interface. e) Perpendicular interfacial anisotropy determined from AHE measurements. The error in this plot arises primarily from the quantification of $M_S$, which we estimate to be less than 10%.

of the OX samples, plotted in blue, follows the FS model up to around 1.8 nm thickness of Pt. However, below this thickness, it deviates from the model. This can occur due to oxygen migration into the Co layer, increasing the resistivity of this layer. Hence, there is a loss of conductance in a very conductive layer of the stack, resulting in the sharp drop at lower thicknesses of Pt. This is also consistent with the magnetization data, exhibiting a loss of magnetic volume around the same thickness of Pt. Moreover, the OX conductance curve crosses the solid red line, which is the limiting case of having no Pt layer. Hence, it is evident that the oxygen migrates from the platinum oxide into the Co layer. As this oxidation of the Co layer occurs before the complete oxidation of the Pt layer, it is indicative of an oxide inversion at the interface, wherein, at lower thicknesses of Pt, oxygen gets pumped into the Co layer, leaving the Pt metallic at the interface.

Based on these data, we propose a generic oxidation model shown in Figure 2c. The plasma oxidizes the top of the Pt layer,[29] enhancing its resistivity. This increase is equivalent to an effective insulating layer of 0.4 nm thick.[21] Moreover, if the Pt is sufficiently thin, the oxygen is not just "pushed" into the Co layer, the Co "attracts" the oxygen from Pt, leaving the interface metallic and hence conductive. This model is different from other works that either assumed a completely oxidized HM layer[17,18] or a completely conducting HM layer.[20] The effect of the metallic Pt at the interface needs to be taken into account while quantifying the SOTs.

To verify this model, we performed ab-initio calculations,[21] in order to determine the energy of the system as the oxygen is placed at different locations in the lattice, as shown in Figure 2d. Here, a plane of oxygen atoms is placed in the lattice along the X-Y plane, and the total energy of the system is calculated by relaxing the structure. By moving this plane of oxygen atoms along the Z direction, we can determine the energy cost of placing oxygen at different locations in Pt and Co. It is evident from this figure that it is energetically more favorable for the oxygen to remain in the Co layer than in the Pt layer. This is also consistent with the enthalpies of formation, mentioned earlier. Hence, near the interface, the oxygen atoms migrate from the Pt layer into the Co layer most likely via grain boundaries.

Now that the distribution of oxygen in Pt has been established, we need to determine the same for the Co layer. We consider the two extreme possibilities: Co oxidized only at the interface or Co oxidized in the bulk, within its entire thickness. In the first case, the reduction of the magnetic moment (Figure 2a) is due to the formation of a magnetic dead layer, while in the second case the thickness is maintained but the $M_S$ is reduced. To find out which of these scenarios is more realistic, we compare the interfacial anisotropy of our samples in both cases. The differences in $M_S$ would be reflected in the interfacial anisotropy, as

$$B_K^{int} = \mu_0 M_S + B_K \quad (1)$$

Here, the perpendicular interfacial anisotropy, $B_K^{int}$, is the difference between the $M_S$, which holds the magnetization of Co in the plane of the sample, and $B_K$, the anisotropy value obtained from the transport measurements of the Anomalous Hall Effect (AHE). These values are plotted in Figure 2e.[21] We find that, within the assumption of dead layer formation, the interfacial anisotropy remains much larger than in the case of uniform oxidation, indicating that the latter is the most plausible scenario. Indeed, it is well established by previous studies of optimized oxidation in Magnetic Tunnel Junctions (MTJ)[30–35] that as the capping layer (Al,[30–32] Mg,[32,33] or Ta[31,32]) is over-oxidized, and the oxygen starts penetrating the Co layer, the perpendicular anisotropy is strongly reduced.[34–36] This is also consistent with the fact that at these thicknesses, Co oxide does not form a passivating layer, leading to bulk oxidation.[37] Hence, in our oxidation model, once the oxygen is pumped into the Co layer, it diffuses into the bulk reducing the $M_S$ of the layer and does not form just an interfacial Co oxide layer.

## 4. Quantifying SOTs Based on the Multi-Layer Oxidation Model

Using the developed oxidation model, the torques are normalized to the current density in platinum and the electric field across it. These are plotted in terms of the corresponding DL-SOT efficiencies as a function of effective Pt thickness in **Figure 3**a,b, respectively. No intrinsic increase in SOTs is observed after thorough corrections and normalizations. Comparing with other published works,[17,18] there is indeed an apparent increase in SOTs at the system level. But after careful consideration of all the measurements, we conclude that there is no new property arising from Pt oxide. Instead, Co is pumping oxygen from the Pt layer, keeping the interface metallic. Moreover, regardless of the type of normalization of SOT efficiency, we obtain the same result highlighting the strength of our model. Following the DL torque normalization, we can perform the same analysis on the FL torques as well. We obtain the same result that there is no intrinsic increase from the oxidation of Pt, as plotted in Figure 3c,d, with overall domination of DL-SOT compared to FL-SOT in agreement with previous reports for Co/Pt interfaces.[38]

Another method of verifying this model is by considering the changes that would occur due to interfacial oxidation. In such a case, the oxygen present at the interface would affect the Rashba field at this interface. This would in turn cause the FL torques to change as they are strongly correlated with the Rashba effect.[39,40] Hence, with increasing oxidation, we would expect FL torque to change significantly compared with the DL torque. However, the opposite is observed wherein the DL and FL torques have the same thickness dependence with Pt. This is plotted in Figure 3e,f, respectively. This strengthens our model of metallic Pt interface and oxygen diffusion within the Co layer. The perfect consistency of our results further proves the importance of controlling the oxidation and understanding the final distribution of oxygen within the stack for determining the real SOT efficiency.

## 5. Conclusion

In conclusion, an apparent increase in torques upon oxidizing platinum is observed, similar to other works. However, this

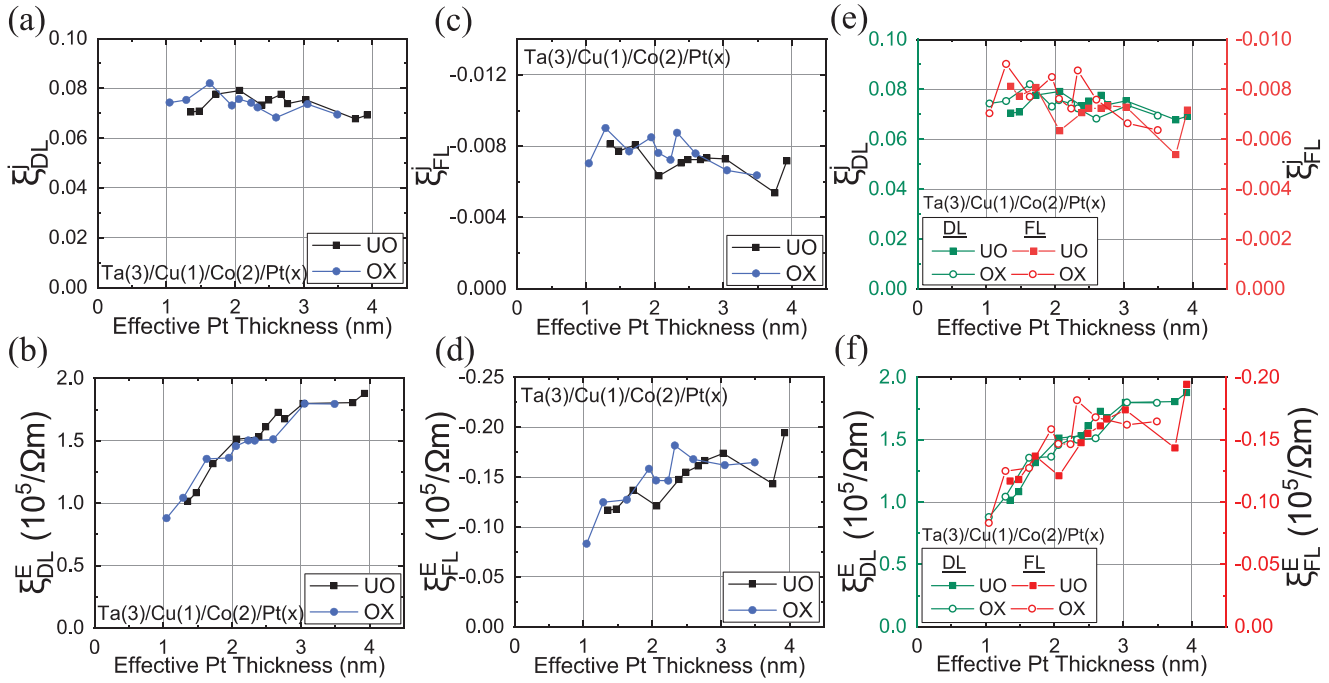


**Figure 3.** DL SOT generation efficiency normalized by a) the current density and b) the applied electric field. FL SOT generation efficiency normalized by c) the current density and d) the applied electric field. Comparison of the DL SOT efficiency and the FL SOT efficiency normalized by e) the current density and f) the applied electric field. The error in these plots is linked to the error in the quantification of the $M_S$ and the current density.

apparent increase disappears when considering a new scenario of HM oxidation in Co/Pt where the HM is no longer completely oxidized but instead oxygen is pumped into the FM, leaving the HM metallic at the interface. This oxygen further diffuses into the bulk of the FM layer affecting its magnetic and electronic properties. These changes of the FM properties are solely responsible for the apparent SOT increase. After appropriate normalizations with resistivity and magnetization we observe no intrinsic increase in torques from the oxidation of the HM. This scenario is validated using ab-initio calculations and $M_S$ and anisotropy measurements. This is likely a general effect: when two oxidized materials are placed in contact with each other, depending on their respective oxide enthalpies of formation, one material could pump oxygen into the other. This needs to be considered in oxidized heterostructures, which are increasingly used in MRAM based applications, in order to avoid erroneous conclusions about key parameters.

## Supporting Information

Supporting Information is available from the Wiley Online Library or from the author.

## Acknowledgements

J.N., E.C., H.Y., E.S., M.A.N., and I.M.M. acknowledge funding for this work from the European Research Council (ERC) under the European Union's Horizon 2020 research and innovation program (Grant Agreement No. 638653—Smart Design). M.S.G. acknowledges funding from MRI-CNCS/UEFISCDI through grant PN-III-P4-ID-PCE-2020-1853.

## Conflict of Interest

The authors declare no conflict of interest.

## Data Availability Statement

The data that support the findings of this study are available from the corresponding author upon reasonable request.

## Keywords

magnetic memory, platinum oxide, Rashba effect, spin hall effect, spin-orbit torques

Received: December 7, 2021
Revised: February 9, 2022
Published online:

[1] J. Ryu, S. Lee, K. Lee, B. Park, *Adv. Mater.* **2020**, *32*, 1907148.
[2] I. M. Miron, K. Garello, G. Gaudin, P.-J. Zermatten, M. V. Costache, S. Auffret, S. Bandiera, B. Rodmacq, A. Schuhl, P. Gambardella, *Nature* **2011**, *476*, 189.
[3] L. Liu, C.-F. Pai, Y. Li, H. W. Tseng, D. C. Ralph, R. A. Buhrman, *Science* **2012**, *336*, 555.
[4] M. Cubukcu, O. Boulle, N. Mikuszeit, C. Hamelin, T. Bracher, N. Lamard, M. C. Cyrille, L. Buda-Prejbeanu, K. Garello, I. M. Miron, O. Klein, G. De Loubens, V. V. Naletov, J. Langer, B. Ocker, P. Gambardella, G. Gaudin, *IEEE Trans. Magn.* **2018**, *54*, 9300204.
[5] C.-F. Pai, L. Liu, Y. Li, H. W. Tseng, D. C. Ralph, R. A. Buhrman, *Appl. Phys. Lett.* **2012**, *101*, 122404.

[6] E. Sagasta, Y. Omori, M. Isasa, M. Gradhand, L. E. Hueso, Y. Niimi, Y. Otani, F. Casanova, *Phys. Rev. B* **2016**, *94*, 060412.
[7] J. W. Lee, Y.-W. Oh, S.-Y. Park, A. I. Figueroa, G. van der Laan, G. Go, K.-J. Lee, B.-G. Park, *Phys. Rev. B* **2017**, *96*, 064405.
[8] M. Obstbaum, M. Decker, A. K. Greitner, M. Haertinger, T. N. G. Meier, M. Kronseder, K. Chadova, S. Wimmer, D. Ködderitzsch, H. Ebert, C. H. Back, *Phys. Rev. Lett.* **2016**, *117*, 167204.
[9] B. Gu, I. Sugai, T. Ziman, G. Y. Guo, N. Nagaosa, T. Seki, K. Takanashi, S. Maekawa, *Phys. Rev. Lett.* **2010**, *105*, 216401.
[10] C.-F. Pai, M.-H. Nguyen, C. Belvin, L. H. Vilela-Leão, D. C. Ralph, R. A. Buhrman, *Appl. Phys. Lett.* **2014**, *104*, 082407.
[11] M.-H. Nguyen, K. X. Nguyen, D. A. Muller, D. C. Ralph, R. A. Buhrman, *Appl. Phys. Lett.* **2015**, *106*, 222402.
[12] W. Zhang, W. Han, X. Jiang, S.-H. Yang, S. S. P. Parkin, *Nat. Phys.* **2015**, *11*, 496.
[13] X. Qiu, W. Legrand, P. He, Y. Wu, J. Yu, R. Ramaswamy, A. Manchon, H. Yang, *Phys. Rev. Lett.* **2016**, *117*, 217206.
[14] Y. Ishikuro, M. Kawaguchi, N. Kato, Y.-C. Lau, M. Hayashi, *Phys. Rev. B* **2019**, *99*, 134421.
[15] A. V. Trifu, *Mesures de Couples de Spin Orbite Dans Des Heterostructures Métal Lourd/Ferromagnet à Base de Pt, Avec Anisotropie Magnétique Planaire*, Université Grenoble Alpes, France, **2017**.
[16] K.-U. Demasius, T. Phung, W. Zhang, B. P. Hughes, S.-H. Yang, A. Kellock, W. Han, A. Pushp, S. S. P. Parkin, *Nat. Commun.* **2016**, *7*, 10644.
[17] H. An, T. Ohno, Y. Kanno, Y. Kageyama, Y. Monnai, H. Maki, J. Shi, K. Ando, *Sci. Adv.* **2018**, *4*, eaar2250.
[18] H. An, Y. Kanno, A. Asami, K. Ando, *Phys. Rev. B* **2018**, *98*, 014401.
[19] A. Asami, H. An, A. Musha, T. Gao, M. Kuroda, K. Ando, *Phys. Rev. B* **2019**, *99*, 024432.
[20] J. Feng, E. Grimaldi, C. O. Avci, M. Baumgartner, G. Cossu, A. Rossi, P. Gambardella, *Phys. Rev. Appl.* **2020**, *13*, 044029.
[21] Supporting information available online.
[22] J. Nath, *Mechanism of Spin-Orbit Torques in Platinum Oxide Systems*, Université Grenoble Alpes, France, **2019**.
[23] I. M. Miron, G. Gaudin, S. Auffret, B. Rodmacq, A. Schuhl, S. Pizzini, J. Vogel, P. Gambardella, *Nat. Mater.* **2010**, *9*, 230.
[24] C.-F. Pai, Y. Ou, L. H. Vilela-Leão, D. C. Ralph, R. A. Buhrman, *Phys. Rev. B* **2015**, *92*, 064426.
[25] J. R. Rumble, *CRC Handbook of Chemistry and Physics : A Ready-Reference Book of Chemical and Physical Data*, CRC Press, Boca Raton, Florida **2019**.
[26] Y. Nagano, *J. Therm. Anal. Calorim.* **2002**, *69*, 831.
[27] K. Fuchs, N. F. Mott, *Math. Proc. Cambridge Philos. Soc.* **1938**, *34*, 100.
[28] E. H. Sondheimer, *Adv. Phys.* **2001**, *50*, 499.
[29] J. J. Blackstock, D. R. Stewart, Z. Li, *Appl. Phys. A* **2005**, *80*, 1343.
[30] S. Monso, B. Rodmacq, S. Auffret, G. Casali, F. Fettar, B. Gilles, B. Dieny, P. Boyer, *Appl. Phys. Lett.* **2002**, *80*, 4157.
[31] B. Rodmacq, S. Auffret, B. Dieny, S. Monso, P. Boyer, *J. Appl. Phys.* **2003**, *93*, 7513.
[32] A. Manchon, C. Ducruet, L. Lombard, S. Auffret, B. Rodmacq, B. Dieny, S. Pizzini, J. Vogel, V. Uhlíř, M. Hochstrasser, G. Panaccione, *J. Appl. Phys.* **2008**, *104*, 043914.
[33] L. E. Nistor, B. Rodmacq, C. Ducruet, C. Portemont, I. L. Prejbeanu, B. Dieny, *IEEE Trans. Magn.* **2010**, *46*, 1412.
[34] H. X. Yang, M. Chshiev, B. Dieny, J. H. Lee, A. Manchon, K. H. Shin, *Phys. Rev. B* **2011**, *84*, 054401.
[35] B. Dieny, M. Chshiev, *Rev. Mod. Phys.* **2017**, *89*, 025008.
[36] A. Hallal, H. X. Yang, B. Dieny, M. Chshiev, *Phys. Rev. B* **2013**, *88*, 184423.
[37] L. Smardz, U. Köbler, W. Zinn, *J. Appl. Phys.* **1992**, *71*, 5199
[38] K. D. Belashchenko, A. A. Kovalev, M. van Schilfgaarde, *Phys. Rev. B* **2020**, *101*, 020407.
[39] A. Kalitsov, S. A. Nikolaev, J. Velev, M. Chshiev, O. Mryasov, *Phys. Rev. B* **2017**, *96*, 214430.
[40] C. O. Pauyac, X. Wang, M. Chshiev, A. Manchon, *Appl. Phys. Lett.* **2013**, *102*, 252403.

 